Molecular Factors Controlling the Isomerization of Azobenzenes in the Cavity of a Flexible Coordination Cage

Supporting information for:

Molecular Factors Controlling the Isomerization of Azobenzenes in the Cavity of a Flexible Coordination Cage

Luca Pesce,[†] Claudio Perego,[†] Angela B. Grommet,[‡] Rafal Klajn,[‡] Giovanni M. Pavan*[,†,¶]

†Department of Innovative Technologies, University of Applied Sciences and Arts of Southern Switzerland, Galleria 2, Via Cantonale 2c, CH-6928 Manno, Switzerland

‡Department of Organic Chemistry, Weizmann Institute of Science, Rehovot 76100, Israel

¶Department of Applied Science and Technology, Politecnico di Torino, Corso Duca degli Abruzzi 24, 10129 Torino, Italy

COMPUTATIONAL METHODS

Parametrization of the atomistic models

The atomistic model of the cage (see Figure 1A) was parametrized according to the GAFF force field.[1] The donor–acceptor (Pd–N) bonds were parametrized using Seminario's method[2] following the Metal Center Parameter Builder (MCPB) protocol.[3] The quantum mechanical calculations were performed using B3LYP functional[4] and, as the basis set, a combination of the DGDZVP set for the palladium atom and the Pople 6-31G* set for the other atoms. The atomistic force field parameters for the metal-bonded parts were extracted from a reduced model of the metal-binding site, consisting of the *cis*-Pd-ligand, the Pd central atom and two Pd-bound imidazole groups (the charge of this reduced system was set to +2, while the multiplicity was set to 1). The partial atomic charges of the whole system were calculated using the RESP approach[5] via Merz-Kollman calculation of the electrostatic potential grid-points on the energy-minimized crystal structure of the cage.[6] The same protocol was applied for the parametrization of AZB, M-AZB, F-AZB and AZP in their *trans*-states. All quantum mechanical calculations were performed using Gaussian-16,[7] while the atomistic parametrization was carried out using the ANTECHAMBER software.[8]

To simulate the photoinduced isomerization of excited molecular switches in the atomistic simulation, we used a molecular model recently employed to study the switching of azobenzene groups within crowded supramolecular assemblies, which correctly reproduces the pathway and kinetics of *trans*→*cis* transition of an excited *trans*-azobenzene (*S**).[9] This model describes *trans* azobenzene units that reached the excited (*S**) state by a modification of the central CNNC dihedral potential term (shown in Figure 4A). The modified dihedral potential induces the spontaneous isomerization of the azobenzenes within picoseconds of classical molecular dynamics (MD) simulations, following the correct out-of-plane rotational pathway[10,11] and according to the expected kinetics for free excited azobenzene.[9,12]

Molecular dynamics simulations

All the atomistic simulations in this work have been conducted using the GROMACS-2018.6 software[13] patched with PLUMED-2.5[14]. All systems were simulated for 1 μs of MD at the temperature of 297 K and pressure of 1 atm in explicit TIP3P water molecules[15] in periodic boundary NPT conditions (constant N: number of particles, P: pressure and T: temperature), employing the v-rescale thermostat[16] and the Berendsen barostat.[17] A timestep of 2 fs was used in the MD simulations unless stated differently. The electrostatic interactions were treated using particle mesh Ewald (PME).[18] The cutoff lengths of the real summation and of the VdW were set to 1.0 nm. The dynamics of the hydrogens was constrained using the LINCS algorithm.[19] In the studies of the *trans*→*cis* transition rates within the cage, the timestep of the simulation was reduced to 0.1 fs in order to guarantee an accurate sampling of the transition.

The starting conformations of all the encapsulated systems were obtained starting from the crystal structure of the system with one cage containing two encapsulated *trans*-F-AZB molecules[6] (CSD entry: TEZLAO[20]). Starting from this complex, we obtained a starting structure of all the other studied *trans* cases by either removing and/or modifying the encapsulated guest and by equilibrating the systems via MD simulation. The initial structures for the *cis* systems were obtained starting from their *trans*-isomers, by triggering their isomerization in the cage and following a MD equilibration.

Metadynamics simulations

In this work, we extensively employed metadynamics (MetaD) simulations[21] to enhance the exploration of the conformational space of the simulated systems. The flexibility of the cage was studied by means of a MetaD simulation using two collective variables (CVs) that are representative of the octahedral structure and along which the MetaD biases the conformational changes of the cage. One CV (CV1) is the distance D1 between the axial palladium atoms in the octahedral cage (red spheres in Figure 2). The other CV (CV2) is the distance D2 between the midpoints of the opposite segments linking the equatorial palladium atoms (green spheres in Figure 2) in the equatorial plane of the cage (see also Figure 1, red and green arrows). During the MetaD run, the bias was deposited along CV1 and CV2 in the form of Gaussian-shaped kernels of height 0.8 kJ/mol and σ equal to 0.05 nm, while the deposition rate was 1 ps^{-1}.

In order to investigate the affinity of encapsulation for each host–guest system, MetaD simulations were performed along two other CVs. One CV (CV1) is the distance between the guest's center-of-mass (COM) from the cage's COM, while the other CV (CV2) is the number of contacts between the guest and the cage. In the cases where the cage contained more than one guest (Figure S4 and Table S3), the MetaD bias was applied only on one of the two guests, while the second one was kept inside the cage by means of a restraint on the number of contacts between the latter and the cage. In these MetaD simulations, the height of the deposited Gaussians was 0.1 kJ/mol (for both CV1 and CV2), and the σ was equal to 0.01 nm along CV1 and 2.0 along CV2. The deposition rate was 1 ps^{-1}.

The estimation of guest residence times were obtained by means of infrequent MetaD simulations,[22–24] following a protocol that allows to reconstruct the unbiased kinetics of rare events triggered by biased simulations. This approach consists of running multiple infrequent well-tempered metadynamics (WT-MetaD)[25] simulations of the host–guest complex, activating/biasing the release of the guests from the host cage[24] by biasing the same CVs used for the MetaD study of the host–guest stability. Here, the bias was deposed every 100 ps using Gaussians of initial height of 2.5 kJ/mol, bias factor of 10, and with the same σs as before. The intrinsic (unbiased) guest expulsion timescales for each system could be then retrieved from the statistics of biased times resulting from multiple infrequent WT-MetaD activating the release of the guests from the cage, and by calculating the transition time distributions.[22–24] The guest expulsion times (t) calculated from multiple WT-MetaD simulations were then used to build the release probability distributions $P_{n\geq1}$ as:

$$P_{n\geq1} = 1 - e^{-\frac{t}{\tau_{off}}} \qquad (1)$$

where τ_{off} is the characteristic timescale for the event of guest release from the cage in the various simulated systems. In all the cases simulated here, the calculated transition time distributions were found to fit well the typical Poissonian distributions expected for rare events (see Figure S5), proving the reliability of the adopted setup. [23,24]

Additionally, the bias computed during these infrequent WT-MetaD simulations could also be used to estimate the free-energy barriers that each system has to overcome in order to have the various guests releasing from the host cage (calculated values for the barriers reported in Figure 5 and Table S2). In particular, the height of the barriers is computed as the height of bias potential accumulated/deposited during infrequent WT-MetaD to trigger the expulsion of the guest. The reported values are the average calculated over the set of infrequent WT-MetaD simulations used for the estimate of τ_{off}. The associated error bar represents the standard deviation of these measurements.

Derivation of thermodynamic and kinetic data

In order to calculate the effective binding affinity between the cage and the guest (ΔG) from the binding free-energy computed from the MetaD simulations (ΔG_{MetaD}), we corrected the latter by accounting for the free-energy contribution due to the concentration of the ligand in the simulation box, as follows:

$$\Delta G = \Delta G_{MetaD} + R\,T \log\left(\frac{[L]}{[L]^0}\right) \qquad (2)$$

where R is the ideal gas constant, T is the temperature of the system in the simulations (297 K), [L] is the concentration of the molecule within the simulation box (Figure 5A: ~ 11.4 mM), and $[L]^0$ is the standard concentration, 1 mol/L.[26]

From ΔG, it is possible to estimate the binding constant K_b as:

$$K_b = \exp\left(-\frac{\Delta G}{RT}\right) \quad (3)$$

where R is the ideal gas constant ($R = 1.987 \times 10^{-3}$ kcal mol^{-1} K^{-1}) and T is the temperature in the simulations (297 K).

The same approach has been followed to calculate from metadynamics simulations the ΔG and K_b for a second guest encapsulation/expulsion in the 2-guests cage containing systems (guest-2 data in Table S3). In these cases, the overall binding constants, K_b(tot), relative to the cumulative encapsulation/expulsion of both guests in/out the cage have been then estimated as: K_b(tot) = K_b(guest-1) × K_b(guest-2) (where the K_b(guest-1) values are reported in Table S1).

Moreover, from the residence time (τ_{off}) estimated by using infrequent WT-MetaD simulations we can compute the k_{off} as:

$$k_{\text{off}} = \frac{1}{\tau_{\text{off}}} \quad (4)$$

Finally, from k_{off} and K_b one can estimate the k_{on} as:

$$k_{\text{on}} = K_b \times k_{off} \quad (5)$$

To obtain the effective binding rate from the k_{on} value (which is measured in units of M^{-1} s^{-1}), it is sufficient to multiply the latter by the guest concentration in the simulated systems (~11.4 mM), as shown in Figure 5A.

Volume analysis

The analysis of the molecular volume of the guests has been performed by using the Mol-Vol code.[27] The radius of the probe was set to 1 Å while the grid step was set to 0.1 Å. In the analysis of Figures 6E,F we changed the σ of the Van der Waals radii of the atoms in the guest in such a way as to obtain an increase of ~5, 10, 20, 30% in the effective volume calculated using Mol-Vol for the various guests.

SUPPLEMENTARY FIGURES AND ADDITIONAL DATA FROM THE MOLECULAR SIMULATIONS

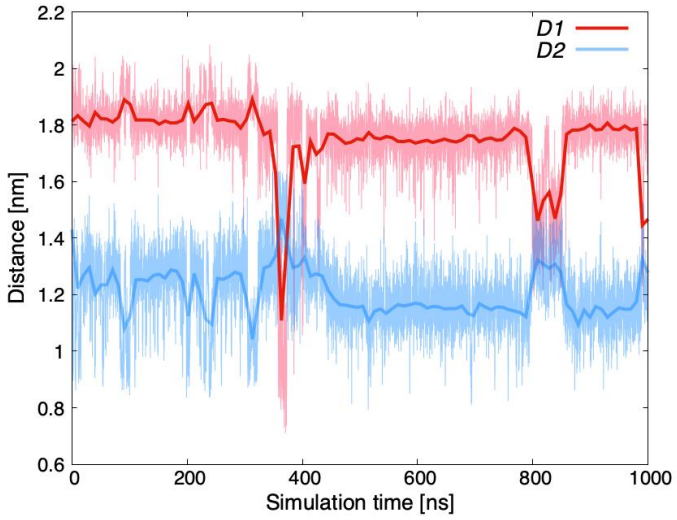

Figure S1: Flexibility of the empty cage. The time-evolution of *D1* (blue) and *D2* (red) for the empty-cage system, along 1 μs of a plain MD simulation. Slow deformation modes of the cage can be detected, although these are rare in the timescales by classical MD. The solid color line is obtained with Bezier smoothing of the raw data (colored in transparency).

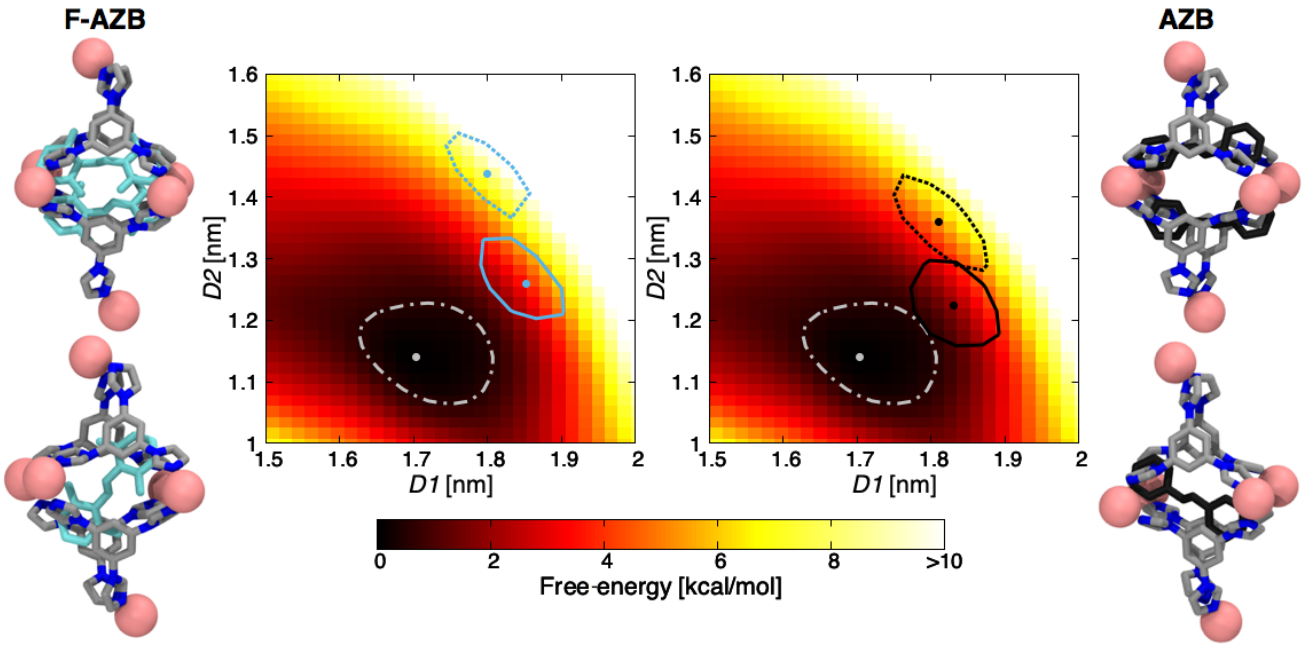

Figure S2: Simultaneous encapsulation of two guests. Equilibrium conformations (in the *D1*–*D2* plane) of the cage upon encapsulation of one and two *trans* guests (F-AZB in cyan, left; AZB in violet, right). For each configuration we report the position of the free-energy minimum (colored dots) and the isolines at 0.5 kcal/mol from the minimum (colored contour lines). The one-guest conformation is indicated by a dot (free-energy minimum) and a solid isoline. The two-guests conformation is indicated by a square (free-energy minimum) and a dot-dashed isoline. These data are projected onto the FES of the empty cage (from Figure 2), for which we report also the minimum and 0.5 kcal/mol isoline (grey dot, dot-dashed isoline). Representative minimum energy configurations for each system are also shown.

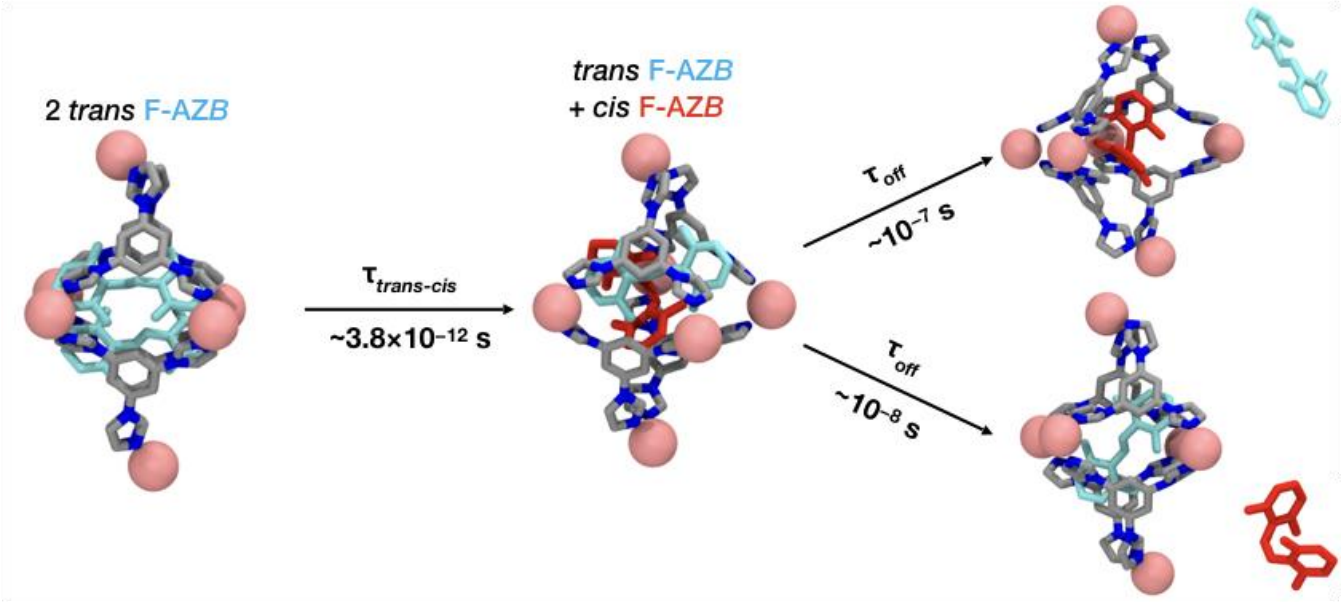

Figure S3: Isomerization inside a cage encapsulating two molecules of *trans*-F-AZB. Soon after isomerization of one encapsulated *trans*-F-AZB guest, one of the two guests leaves the cage. On average, release out from the cage of the *cis*-isomer (red) is ~10 times more frequent/probable (residence time of $\sim 10^{-8}$ s) than release of the *trans*-isomer (cyan; residence time $\sim 10^{-7}$ s).

Table S1: Equilibrium constants for host–guest complex formation, K_b, and kinetic constants for the expulsion and encapsulation of the guest (k_{off} and k_{on}, respectively).

Guest	State	K_b [M^{-1}]	k_{off} [s^{-1}]	k_{on} [$M^{-1}\,s^{-1}$]
AZB	*trans*	7.87×10^3	2.65×10^3	2.1×10^7
AZB	*cis*	1.66×10^5	7.81×10^3	1.3×10^9
M-AZB	*trans*	6.41×10^5	8.3×10^1	5.3×10^7
M-AZB	*cis*	4.24×10^4	2.85×10^2	1.2×10^7
F-AZB	*trans*	7.87×10^3	2.63×10^2	2.1×10^6
F-AZB	*cis*	4.55×10^2	1.56×10^3	7.0×10^5
AZP	*trans*	1.55×10^4	2.38×10^3	3.7×10^7
AZP	*cis*	2.78×10^5	5.46×10^3	1.5×10^9

Table S2: Binding free-energies (ΔG), free-energy barriers for guest expulsion, and guest residence times within the cage.

Guest	State	ΔG [kcal/mol]	Barrier [kcal/mol]	τ_{off} [s]
AZB	*trans*	-5.3 ± 1.3	8.7 ± 1.3	$(3.9 \pm 0.2) \times 10^{-4}$
AZB	*cis*	-7.1 ± 1.4	7.9 ± 1.3	$(1.28 \pm 0.06) \times 10^{-4}$
M-AZB	*trans*	-7.9 ± 2.5	11.0 ± 1.0	$(1.2 \pm 0.1) \times 10^{-2}$
M-AZB	*cis*	-6.3 ± 0.3	8.2 ± 1.2	$(3.5 \pm 0.3) \times 10^{-3}$
F-AZB	*trans*	-5.3 ± 1.8	10.1 ± 1.0	$(3.8 \pm 0.1) \times 10^{-3}$
F-AZB	*cis*	-3.6 ± 0.8	8.6 ± 0.9	$(6.4 \pm 0.2) \times 10^{-4}$
AZP	*trans*	-5.7 ± 2.0	8.4 ± 1.0	$(4.2 \pm 0.1) \times 10^{-4}$
AZP	*cis*	-7.4 ± 0.3	8.1 ± 1.0	$(1.83 \pm 0.05) \times 10^{-4}$

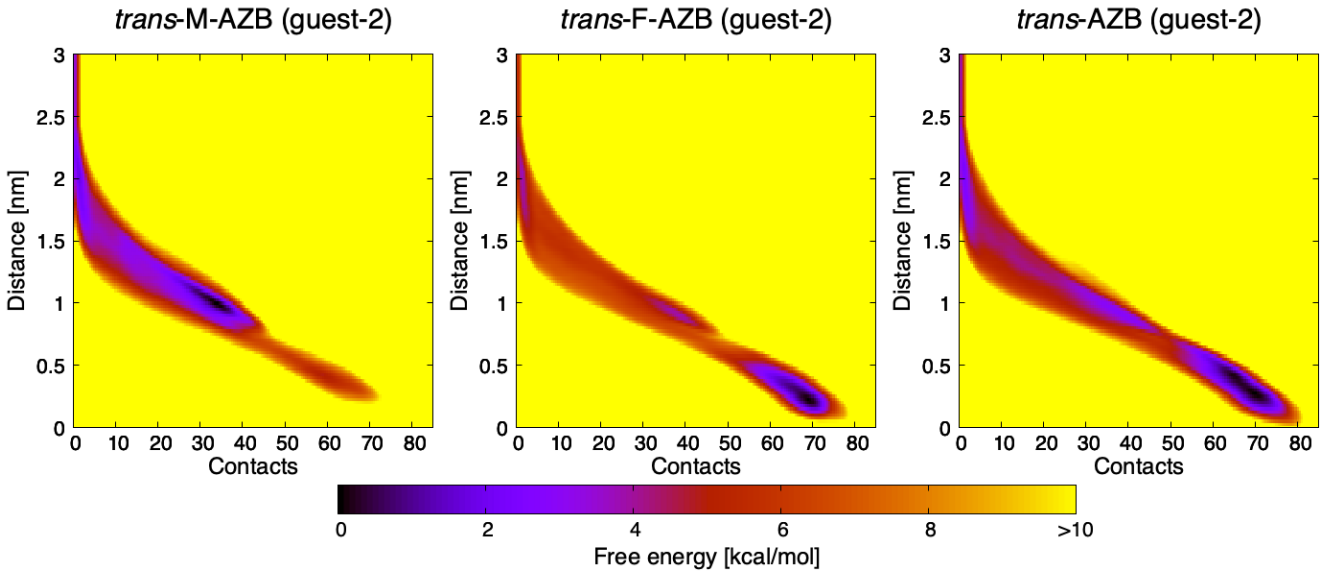

Figure S4: Limits of guest encapsulation. Free-energy surfaces (FES) of related to the encapsulation/release of the second *trans*-M-AZB (left), *trans*-F-AZB (center) or *trans*-AZB (right) guest (guest-2), in/out a cage containing the first bound (*trans*-M-AZB, *trans*-F-AZB, or *trans*-AZB) guest (guest-1). Dark colors in the FES identify minimum energy configurations for the systems. The FESs demonstrate that, while the incorporation of a second *trans*-F-AZB guest or of a second *trans*-AZB guest inside the cage is an energetically favored event, the cage cannot accommodate two *trans*-M-AZB guests at the same time. In this case, the most favorable state for the second *trans*-M-AZB is at 1 nm from the center of the cage – *i.e.*, adsorbed on the cage surface.

Table S3: Binding free-energies (ΔG(guest-2)) and equilibrium binding constants (K_b(guest-2)) for the incorporation/release of a second *trans* guest in/out the cage, and overall binding constants (K_b(tot)) of the two-guests complexes.

Guest	State	ΔG(guest-2) [kcal/mol] [a]	K_b(guest-2) [M^{-1}] [a]	K_b(tot) [M^{-2}] [b]
AZB	*trans*	-6.2 ± 0.7	3.7×10^4	0.3×10^9
F-AZB	*trans*	-7.1 ± 0.9	1.66×10^5	1.3×10^9

[a] Thermodynamic and kinetic data obtained from metadynamics simulation exploring encapsulation/release of the second *trans* guest in/out the cage while the first *trans* one remains encapsulated inside the cavity. [b] Overall binding constant, K_b(tot), relative to the cumulative encapsulation/release of two *trans* guests in/out the cage. The K_b(tot) values were calculated from metadynamics simulations (same procedure of the single-guest simulations described above) activating the encapsulation/release of the second *trans* guest (guest-2) in/out a cage containing the first encapsulated *trans* guest (guest-1) (see Figure S4). The K_b(tot) values have been then estimated as: K_b(tot) = K_b(guest-1) × K_b(guest-2) (see Table S1 for the K_b(guest-1) values). For the case of the cage encapsulating two *trans*-AZB guests, the global K_b(tot) value estimated from the metadynamics simulations was found consistent with that available from the experiments (on the order of ~10^9 M^{-2}).[6]

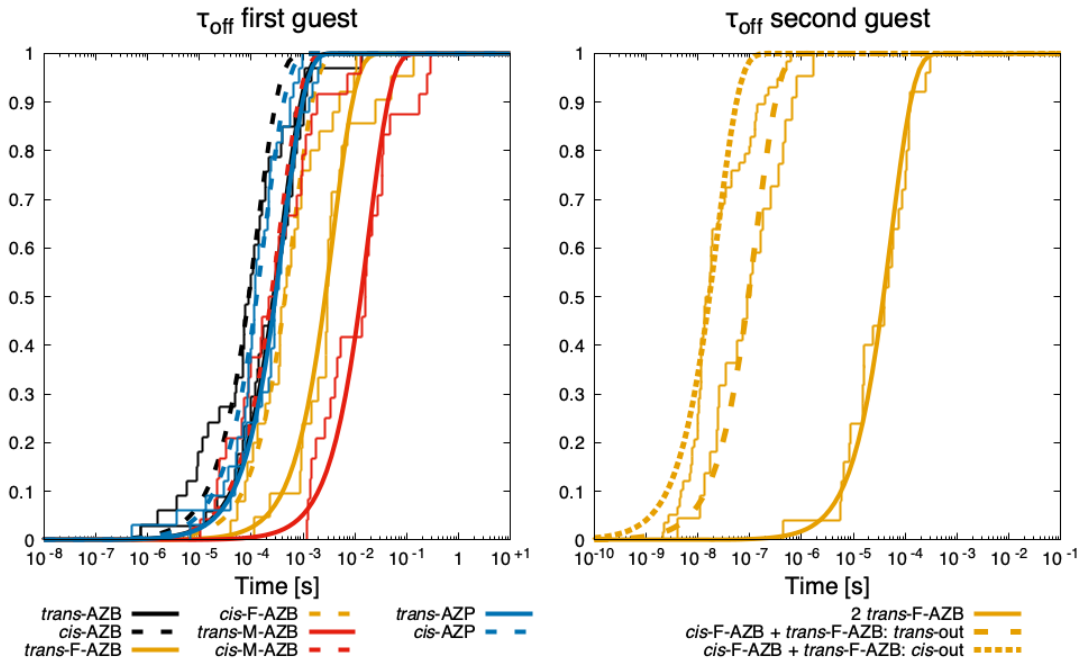

Figure S5: Estimation of guest residence time. Cumulative expulsion probability distributions $P_{n\geq 1}$ obtained by fitting the guest release times calculated from the infrequent WT-MetaD simulations. From these distributions it is possible to calculate the characteristic residence times τ_{off} (Eq. 1). Residence timescales (or, the characteristic expulsion timescales) for guests outside the cage during single-guest encapsulation (left panel): for each set of data we report the individual expulsion times obtained by individual infrequent WT-MetaD runs for each case (colored segments) and the Poissonian fit (solid or dashed sigmoidal curves) from which we can estimate of the guest residence time in the cage τ_{off}. Right panel: guest expulsion kinetics for one of the two encapsulated F-AZB guests in the cage before excitation (solid line) or after transition of one of the two F-AZB guests has occurred. Dotted line: release of *cis*-F-AZB from the cage (faster); dashed line: release of *trans*-F-AZB from the cage (slower).

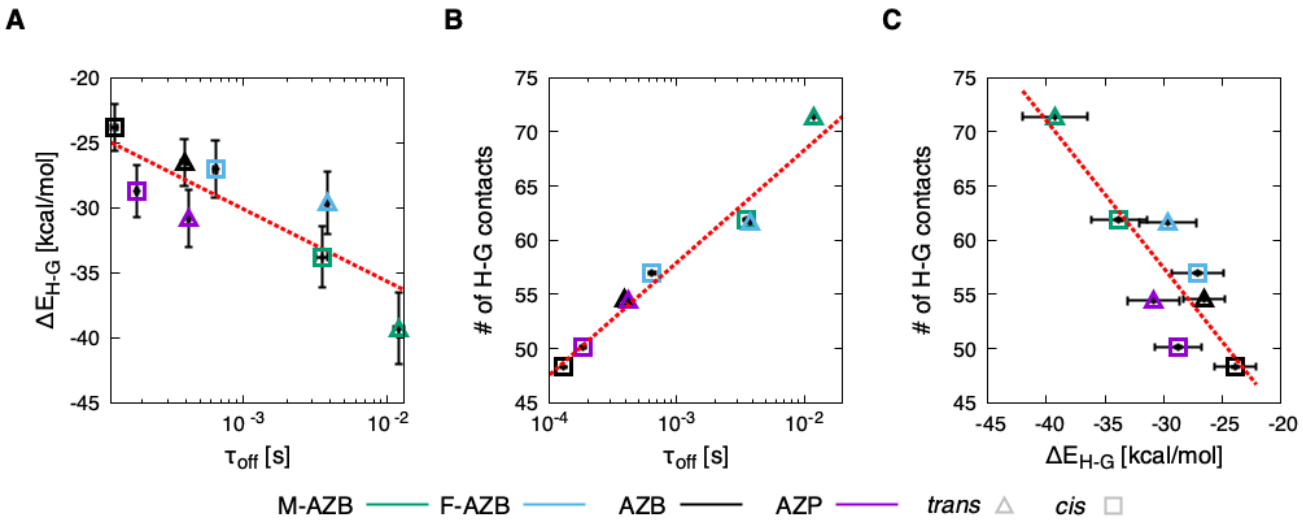

Figure S6: Host–guest interactions and crowding effects *vs.* residence time. **A** Relationship between guest residence time τ_{off} and host–guest interaction energy ΔE_{HG}. Data are reported for *trans* (triangles) and *cis* guests (squares); on average the interaction with the cage is stronger for *trans* than for *cis* guests. **B** Relationship between τ_{off} and the number of contacts (calculated considering only the heavy atoms) between host and guest. This data, indicative of crowding in the cavity, indicates that crowding is generally higher for *trans* than for *cis* guests. **C** Relationship between ΔE_{HG} and the number of contacts between the host and the guest. The error bars indicate the standard deviation of the data.

SUPPLEMENTARY REFERENCES

(1) Wang, J.; Wolf, R. M.; Caldwell, J. W.; Kollman, P. A.; Case, D. A. Development and Testing of a General Amber Force Field. *J. Comput. Chem.* **2004**, *25*, 1157–1174.

(2) Seminario, J. M. Calculation of Intramolecular Force Fields from Second-Derivative Tensors. *Int. J. Quantum Chem.* **1996**, *60*, 1271–1277.

(3) Li, P.; Merz, K. M. MCPB.Py: A Python Based Metal Center Parameter Builder. *J. Chem. Inf. Model.* **2016**, *56*, 599–604.

(4) Becke, A. D. Density-Functional Thermochemistry. III. The Role of Exact Exchange. *J. Chem. Phys.*, **1993**, *98*, 5648–5652.

(5) Bayly, C. I.; Cieplak, P.; Cornell, W.; Kollman, P. A. A Well-Behaved Electrostatic Potential Based Method Using Charge Restraints for Deriving Atomic Charges: The RESP Model. *J. Phys. Chem.* **1993**, *97*, 10269–10280.

(6) Samanta, D.; Gemen, J.; Chu, Z.; Diskin-Posner, Y.; Shimon, L. J. W.; Klajn, R. Reversible Photoswitching of Encapsulated Azobenzenes in Water. *Proc. Natl. Acad. Sci. USA* **2018**, *115*, 9379–9384.

(7) Frisch, M. J.; Trucks, G. W.; Schlegel, H. B.; Scuseria, G. E.; Robb, M. A.; Cheeseman, J. R.; Montgomery; Jr.; J. A.; Vreven, T.; et al. *Gaussian 03*; Gaussian, Inc.: Wallingford, CT, 2004.

(8) Wang, J.; Wang, W.; Kollman, P.; Case, D. ANTECHAMBER: An Accessory Software Package for Molecular Mechanical Calculations. *J. Chem. Inf. Comp. Sci.* **2000**, *222*.

(9) Bochicchio, D.; Kwangmettatam, S.; Kudernac, T.; Pavan, G. M. How Defects Control the Out-of-Equilibrium Dissipative Evolution of a Supramolecular Tubule. *ACS Nano* **2019**, *13*, 4322–4334.

(10) Tiago, M. L.; Ismail-Beigi, S.; Louie, S. G. Photoisomerization of Azobenzene from First-Principles Constrained Density-Functional Calculations. *J Chem Phys* **2005**, *122*, 094311.

(11) Pederzoli, M.; Pittner, J.; Barbatti, M.; Lischka, H. Nonadiabatic Molecular Dynamics Study of the *cis–trans* Photoisomerization of Azobenzene Excited to the S_1 State. *J. Phys. Chem. A* **2011**, *115*, 11136–11143.

(12) Cantatore, V.; Granucci, G.; Rousseau, G.; Padula, G.; Persico, M. Photoisomerization of Self-Assembled Monolayers of Azobiphenyls: Simulations Highlight the Role of Packing and Defects. *J. Phys. Chem. Lett.* **2016**, *7*, 4027–4031.

(13) Hess, B.; Kutzner, C.; van der Spoel, D.; Lindahl, E. GROMACS 4: Algorithms for Highly Efficient, Load-Balanced, and Scalable Molecular Simulation. *J. Chem. Theory Comput.* **2008**, *4*, 435–447.

(14) Tribello, G. A.; Bonomi, M.; Branduardi, D.; Camilloni, C.; Bussi, G. PLUMED 2: New Feathers for an Old Bird. *Comput. Phys. Commun.* **2014**, *185*, 604–613.

(15) Jorgensen, W. L.; Chandrasekhar, J.; Madura, J. D.; Impey, R. W.; Klein, M. L. Comparison of Simple Potential Functions for Simulating Liquid Water. *J. Chem. Phys.* **1983**, *79*, 926–935.

(16) Bussi, G.; Donadio, D.; Parrinello, M. Canonical Sampling through Velocity Rescaling. *J. Chem. Phys.* **2007**, *126*, 014101.

(17) Berendsen, H. J. C.; Postma, J. P. M.; van Gunsteren, W. F.; DiNola, A.; Haak, J. R. Molecular Dynamics with Coupling to an External Bath. *J. Chem. Phys.* **1984**, *81*, 3684–3690.
(18) Essmann, U.; Perera, L.; Berkowitz, M. L.; Darden, T.; Lee, H.; Pedersen, L. G. A Smooth Particle Mesh Ewald Method. *J. Chem. Phys.* **1995**, *103*, 8577–8593.
(19) Hess, B.; Bekker, H.; Berendsen, H.; Fraaije, J. LINCS: A Linear Constraint Solver for Molecular Simulations. *J. Comput. Chem.* **1998**, *18*, 1463–1472.
(20) Groom, C. R.; Bruno, I. J.; Lightfoot, M. P.; Ward, S. C. The Cambridge Structural Database. *Acta Crystallogr. B* **2016**, *72*, 171–179.
(21) Laio, A.; Parrinello, M. Escaping Free-Energy Minima. *Proc. Natl. Acad. Sci. USA* **2002**, *99*, 12562–12566.
(22) Tiwary, P.; Parrinello, M. From Metadynamics to Dynamics. *Phys. Rev. Lett.* **2013**, *111*, 230602.
(23) Salvalaglio, M.; Tiwary, P.; Parrinello, M. Assessing the Reliability of the Dynamics Reconstructed from Metadynamics. *J. Chem. Theory Comput.* **2014**, *10*, 1420–1425.
(24) Bochicchio, D.; Salvalaglio, M.; Pavan, G. M. Into the Dynamics of a Supramolecular Polymer at Submolecular Resolution. *Nat. Commun.* **2017**, *8*, 147.
(25) Barducci, A.; Bussi, G.; Parrinello, M. Well-Tempered Metadynamics: A Smoothly Converging and Tunable Free-Energy Method. *Phys. Rev. Lett.* **2008**, *100*, 020603.
(26) Kranjc, A.; Bongarzone, S.; Rossetti, G.; Biarnés, X.; Cavalli, A.; Bolognesi, M. L.; Roberti, M.; Legname, G.; Carloni, P. Docking Ligands on Protein Surfaces: The Case Study of Prion Protein. *J. Chem. Theory Comput.* **2009**, *5*, 2565–2573.
(27) NAMD was developed by the Theoretical Biophysics Group in the Beckman Institute for Advanced Science and Technology at the University of Illinois at Urbana–Champaign.